# Optical Counterparts of Galactic Supernova Remnants and their Kinematic Distances

**Margarita Rosado (IA-UNAM), Mónica Sánchez-Cruces (LAM, France), Patricia Ambrocio-Cruz (ITSOEH, México), Diego Trejo (FC-UNAM).**


## ABSTRACT

Optical counterparts of Galactic supernova remnants (SNRs) are identified by high [SII]/Hα line-ratios characteristic of radiative shock emission. Sometimes it is the only line emission of the SNR and thus, the only means of getting the SNR kinematical distance. We present results of optical observations in the lines of Hα and [SII] (λλ 6717 and 6731 Å) obtained with the UNAM Scanning Fabry-Perot Interferometer PUMA aimed at obtaining the kinematical distance, shock velocity and other important parameters of two SNRs with optical counterparts. We discuss on how kinematical distances agree with other distance determinations. The studied SNRs are CTB 109 hosting a magnetar and the SNR IC 443.


## Introduction

In our Galaxy, there are about 274 SNRs (Green 2009) catalogued by their radio emission, of which only about 29% have optical counterparts (Green 2014; Stupar & Parker 2011).

Much research has been performed on this subset of objects because optical data complement studies at other wavelengths and allow us to determine the physical and chemical conditions of the SNRs as well as their distances, because of the existence of optical emission lines, such as Hα or [SII]6717 Å that allow us to measure the Doppler shift of the lines; however, optical kinematic data are scarce. We have started a survey of Galactic SNRs in the northern hemisphere of the Galaxy with optical counterparts using the UNAM scanning Fabry-Perot (FP) interferometer PUMA surveying the [SII] (λλ 6717 and 6731 Å) and Hα lines. This provides us a homogeneous set of data from SNRs as well as from their environment. These data are important for the accurate determination of kinematic distances to these objects. Indeed, one of the aims of this project is to establish reliable kinematic distances for SNRs, and this determination require a large sample of data.

## Observations and Data Reduction

Observations were made with the f/7.5 Cassegrain focus of the 2.1m telescope from the Observatorio Astronómico Nacional of the Universidad Nacional Autónoma de México, at San Pedro Mártir, B. C., Mexico using the UNAM scanning Fabry-Perot interferometer PUMA (Rosado et al. 1995). We used a 2048 × 2048 pixels Marconi CCD detector with a binning factor of 4, obtaining a field of view of 10’ with a spatial sampling of 1”.3/px. The Fabry-Perot sampling spectral resolution is 0.41 Å at Hα (equivalent to 19.0 km/s), free spectral range of 19.8 Å (equivalent to a velocity range of 908 km /s).

We obtained direct images of the optical counterparts of the SNRs in Hα and [SII] using the PUMA focal reducer without the Fabry-Perot interferometer in the instrument optical axis. We also obtained [SII] (λλ6717,6731 Å) Fabry-Perot data cubes of regions of the SNRs CTB 109 and IC 443. We scan the FP interferometer through 48 channels, with integration time of 120s per channel obtaining object data cubes of dimensions 512 × 512 × 48.

Data reduction has been achieved by means of the software CIGALE which allows flat field correction, wavelength and absolute flux calibration, construction of the velocity maps and radial velocity profile extraction and fitting. Further details are described in Sánchez-Cruces et al. (2018).

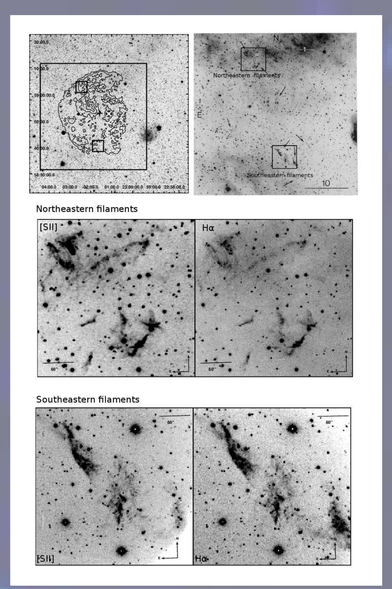


Fig. 1. Top-left: DSS image overplotted the X-ray emission from ROSAT. Big box indicates the size Hα image of Fesen & Hurford (1995) field, small boxes show the filaments regions studied in this work. Top-right: Remnant field showing Hα image taken from Fesen & Hurford (1995). Bottom: Hα (right) and [SII] (left) direct images obtained with PUMA from NE and SE filaments.

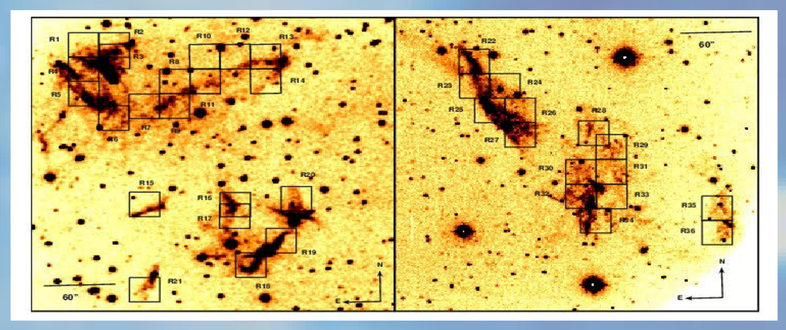

Fig. 2 [SII] direct images showing the regions in which we divided the filaments in order to carry out our analysis (R1 to R36). Left and right panels correspond to the Northeastern and Southeastern filaments, respectively.

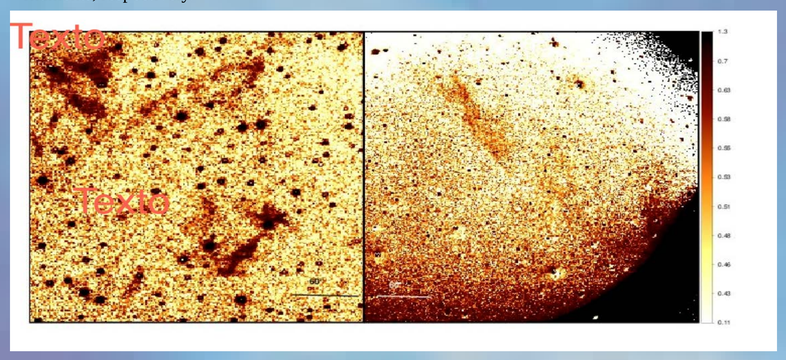

Fig. 3 SII]/Hα map of Northeastern (left) and Southeastern (right) filaments of the SNR G109.1-1.0. It is shown that the [SII]/Hα line ratio values are larger than 0.5, characteristic of SNRs.

## Results

### CTB 109

The supernova remnant G109.1-1.0 (CTB109) is located at α(J 2000) =23h 01m 35s , δ(J 2000) =+58◦ 53’ according to their source centroid (Green Catalog, Green 2014). Its morphology is shell-like and it shows a semicircular shell both in X-ray (Gregory & Fahlman 1980) and radio emission. The Hα emission of this remnant presents filamentary structure found by Fesen & Hurford (1995). Also, some studies reveal that molecular and atomic material are interacting with the SNR (see Tatematsu et al. 1987, Kothes et al. 2002, Sasaki et al. 2006, Tian et al. 2010, Kothes & Foster 2012). There is a strong correlation between X-ray emission and radio emission and that the X-ray pulsar AXP 1E 2259+586 (marked with a “×”) and the geometric center (marked with “+”) are not coincident suggesting a transverse motion of the anomalous X-ray pulsar. The anomalous X-ray pulsar (AXP) 1E 2259+586 hosted in CTB 109 is a magnetar listed as MG J2301+5852 in the McGill magnetar catalog (Olausen & Kaspi 2014) and as AXP J2301+5852. In Sánchez-Cruces et al. (2018):

1.- We have classified 6 Hα filaments, three of them classified previously by Fesen & Hurford (1995). We have confirmed that these Hα filaments are indeed the optical counterpart of the radio SNR by finding high [SII]/Hα line-ratios, characteristic of shocked regions of SNRs.

2. We also estimated the radial velocity components referred to the LSR for each filament. We found that the systemic velocity of the SNR is VLSR=-50±6 km/s. This result is in agreement with other estimates of the SNR distance based in CO and HI kinematic distances of other objects presumed to be near the SNR. With this radial velocity we estimated a distance to the SNR CTB 109 of 3.1±0.2 kpc following the distance-velocity diagram toward CTB109 of Foster & MacWilliams (2006), placing the SNR in the Perseus Arm. This value is in agreement with the distance to the magnetar estimated using its dispersion (DM) value.

3. We obtained a expansion velocity of this supernova remnant of about $V_{exp}$=230±5 km/s.

4. Using the [SII]λ6717/[SII]λ6731 ratios we found an electron density of $n_e$ = 580 $cm^{-3}$ . We estimate a initial energy similar to the energies deposited by normal supernovae.Thus a magnetar does not release larger amounts of mechanical energy to the medium.

**This work is supported by grants 253085 from CONACYT and IN109919 from DGAPA-UNAM**

5. The age of the SNR computed here is 9000 yr in agreement with the age estimated for the magnetar by Tendulkar et al. (2013). This agreement is important because magnetars cannot be detected with longer ages due to their magnetic field decay. The initial energy deposited in the ISM by the SN explosion derived in this work is $E_0$=1.8 to 5.2 × $10^{50}$ erg (depending on whether the SNR is in the Sedov or the radiative phase of evolution) which is not different from the energy deposited by a supernova forming a pulsar. This suggests that it is not possible to identify supernovae forming magnetars from supernovae forming typical pulsars from the energies deposited in the ISM.

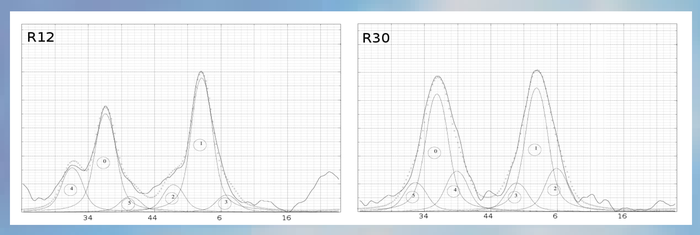


Fig. 4 [SII] radial velocity profiles of two regions obtained with FP. The profiles were integrated over boxes of 20 × 20 pixel size. The x-axis in the profiles gives the λ channels and the y-axis is the intensity in arbitrary units. Both [SII] lines at 6717 Å and 6731 Å are detected. Decomposition of each profile is indicated in thin lines. Resulting profile is shown as hollow circles and with numbers. Dotted line represent the sum of all fitted components.

## Results

### IC 443

The well known SNR IC 443 had not until quite recently a well determined distance. Indeed, the optical studies based on obtaining systemic velocities in order to get kinematic distances reported distances between 0.7 kpc to 1.5 kopc. While the assumption that the SNR is associated with the HII región S249 located it at a distance of 1,5-2 kpc. This latter distance is based on the photometric distance of exciting stars of S249 that belong to the stellar association GemOB1. In Ambrocio-Cruz et al. (2017) we were able of obtaining the kinematics of both the SNR IC 443 and the HII región S249. These studies enable us to distinguish between the SNR and the HII region S249, both of which are in the line of sight. Indeed, all the velocity profiles have a narrow width velocity component due to the HII region emission plus the contribution of the SNR present as complex and wider velocity components as can be appreciated in Table 5 from that work. From this we were able of determining the kinematic distances of the SNR and the HII region and we find that the HII region is located 0.6 kpc in front of the SNR.

We also determined the expansión velocity and energy deposited in the interstellar medium due to the SN explosión.

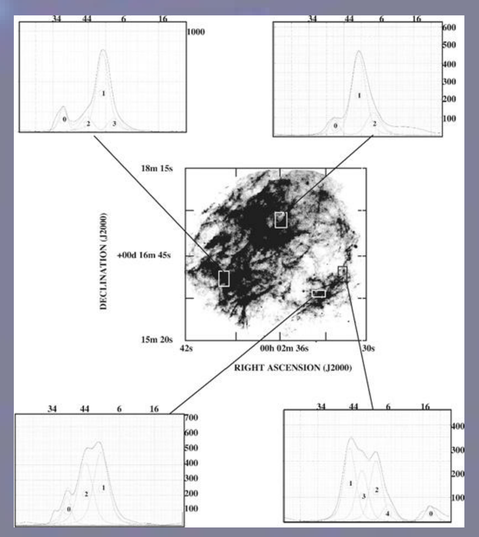


Fig. 5. Radial velocity profiles integrated over various areas of the NE región of the Galactic SNR IC 443.The vertical axis is the intensity in arbitrary units, the horizontal axis is the velocity cannel number. The filaments show violent motions some with Vexp > 100 km/s. Taken from Ambrocio-Cruz et al. 2017.

**Table 1. Main Derived Properties of the SNRs**

| SNR Name | $V_{LSR}$ (km/s) | distance (kpc) | R (pc) | $V_{EXP}$ (km/s) | Age ($10^4$ yr) | $n_0$ ($cm^{-3}$) | $E_0$ ($10^{50}$ erg) |
|---|---|---|---|---|---|---|---|
| CTB109 | -50 | 3.1 | 14 | 230 | 0.9 | 1.1 | 1.8-5.2 |
| IC 443 | +9 | 1.9 | 10.5 | 105 | 3.0 | 10 | 7.2 |

### References

Ambrocio-Cruz et al. 2014, RMxAA 50, 323, Ambrocio-Cruz et al. 2017, MNRAS 472, 51, Fesen & Hurford 1995, AJ 110, 747, Foster & MacWilliams 2006, ApJ 644, 214, Green 2014, BAS India 42, 47, Gregory & Fahlman 1985, Nature 287, 805, Holden 1968, MNRAS 141, 57, Kothes et al., 2002, NS in SNRs 271, 205, Kothes & Foster 2012, ApJ 746, L4, Olausen & Kaspi 2014, ApJS 212, 6, Rosado 1982, RMxAA 5, 127, Rosado et al. 1995, RMxAASC 3, 263, Sánchez-Cruces et al. 2018, MNRAS 473,1705 .,Sasaki et al. 2006, ApJ 642, L149, Stupar & Parker 2011, MNRAS 414, 2282, Tatematsu et al. 1987, A&A 184, 279, Tian et al. 2010, MNRAS 404, L1.